Vortices in trapped alkali BECs

Dimitrios Galanakis

8th May 2002

Abstract

This essay presents a very brief review of the theory of the Bose Einstein condensation in alkali gases concentrating more in the description of vortices and vortex lattices and also in their recent experimental observation.

1 Introduction

Bose-Einstein condensations was directly observed for the first time in trapped alkali gasses in 1995 in a series of Rb (Anderson et. al.) and Na (Davis et. al.) experiments in which the atoms were confined in appropriate magnetic traps and cooled down to extremely low temperatures of fractions of microkelvins. The condensate was identified by the existence of a sharp peak in the velocity distribution bellow a certain critical temperature. Although the existence of BE condensation was predicted long ago and it was accosiated with will known phenomena such as superfluidity and superconductivity the achievements in the creation of an almost novel BEC system renewed the theoretical and experimental interest.

One of the most intriguing characteristics of BECs is the existence of persistent currests that are associated with vortices which are phase signularities of topological character. In this paper we are going to present the standard technology that is used to treat the vortexes in BEC, the Gross Pitaevskii equation, and we are going to present experimental observations of vortices and vortex lattices in alkali BECs.

2 Trapped alkali gasses

Contemporary experiments use sophisticated techiniques to trap a dilute alkali gas of about $10^4 - 10^7$ atoms, such as laser and mangetic traps. Most of these traps are simulating a harmonic potential. which is of the form:

$$V_{tr}(\mathbf{r}) = \frac{m}{2}(\omega_x^2 x^2 + \omega_y^2 y^2 + \omega_z^2 z^2) \tag{1}$$

If we neglect the interparticle interaction the energy of the system is obviously:

$$\varepsilon_{n_x n_y n_z} = \left(n_x + \frac{1}{2}\right)\hbar\omega_x + \left(n_y + \frac{1}{2}\right)\hbar\omega_y + \left(n_z + \frac{1}{2}\right)\hbar\omega_z \ , \tag{2}$$

where $\{n_x, n_y, n_z\}$ are non-negative integers. The ground state $\phi(\mathbf{r}_1, .., \mathbf{r}_N)$ of N noninteracting bosons confined by the potential (1) is obtained by putting all the particles in the lowest single-particle state ($n_x = n_y = n_z = 0$):

$$\varphi_0(\mathbf{r}) = \prod_i \varphi_0(\mathbf{r}_i) = \left(\frac{m\omega_{\rm ho}}{\pi\hbar}\right)^{3/4} \exp\left[-\frac{m}{2\hbar}(\omega_x x^2 + \omega_y y^2 + \omega_z z^2)\right] \tag{3}$$

where $\omega_0 = (\omega_x\omega_y\omega_z)^{1/3}$ is the geometric average of the oscillator frequencies. The density distribution then becomes $n(\mathbf{r}) = N|\varphi_0(\mathbf{r})|^2$ and its value grows with N. The size of the cloud is instead independent of N and is given by $d_0 = \left(\frac{\hbar}{m\omega_{\rm ho}}\right)^{1/2}$ it corresponds to the standard deviation of the Gaussian (3). and for an alkali gas is of the order of 1μm. At finite temperature only part of the atoms occupy the lowest state, the others being thermally distributed in the excited states at higher energy. It can be shown that the radious of the thermaly excited states is larger than d_0. As an approximation lets assume that $k_BT \gg \hbar\omega_0$ and approximate the density of the excited states with a classical Boltzmann distribution $n_{\rm cl}(r) \propto \exp[-V_{tr}(r)/k_BT] = \exp[-\frac{1}{2k_BT}m\omega_0^2 r]$ which is a Gaussian with width $R_T = d_0(k_BT/\hbar\omega_0)^{1/2}$ larger than $a_{\rm ho}$.

Note that the Fourier transform of 3 is a Gaussian with width $d_i^{-1} = \left(\frac{\hbar}{m\omega_i}\right)^{-1/2}$ in the i^{th} direction and the width of the excited states is still broader and proportional to $(k_BT)^{1/2}$. We see that Bose-Einstein condensation in harmonic traps shows up with the appearance of a sharp peak in the central region of the density distribution both in momentum and coordinate space whereas in a uniform gas the peak is evident only in momentum space. This is actually a unique characteristic of trapped gasses which has importan implications both in the experimental and theoretical analysis. Actually the initialy detection of BEC was done both in velocity and coordinate space. In the former case, for a non interacting gas, the trap is switched off and the expantion of the condensate is almost ballistic. The velocities of the particles are determined from the time of flight. In the latter the distribution of the atoms is measured directly using light scattering techniques. The theoretical challenge is to study the effect of two-body interactions in the shape of the distribution.

Another important aspect is the symmetry of the confining potential. In this essay we are going to deal only with axis-symmetric potentials of the form $V_{tr}(\mathbf{r}) = \frac{m}{2}(\omega_\perp^2 r_\perp^2 + \omega_z^2 z^2)$ where z is the axial and $r_\perp = (x^2 + y^2)^{1/2}$ is the radial coordinate. Usually we characterize the assymetry of the trap by the ratio $\lambda = \omega_z/\omega_\perp$which for $\lambda < 1$ corresponds to a cigar-shaped trap while for $\lambda > 1$ to a disk-shaped . In terms of λ the ground state (3) for noninteracting bosons can be rewritten as

$$\varphi_0(\mathbf{r}) = \frac{\lambda^{1/4}}{\pi^{3/4} a_\perp^{3/2}} \exp\left[-\frac{1}{2d_\perp^2}(r_\perp^2 + \lambda z^2)\right] . \tag{4}$$

Here $d_\perp = (\hbar/m\omega_\perp)^{1/2}$ is the harmonic oscillator length in the x-y plane and, since $\omega_\perp = \lambda^{-1/3}\omega_0$, one has also $d_\perp = \lambda^{1/6} d_0$.

The choice of an axially symmetric trap has proven useful for providing further evidence of Bose-Einstein condensation from the analysis of the momentum distribution. The Fourier transform of the wave function (4) is $\tilde{\varphi}_0(\mathbf{p}) \propto \exp[-d_\perp^2(p_\perp^2 + \lambda^{-1}p_z^2)/2\hbar^2]$. The ration of tha axial and radial widths is $\sqrt{\langle p_z^2\rangle/\langle p_\perp^2\rangle} = \sqrt{\lambda}$ and is determined only by the asymmetry of the trap. Thus, the shape of the condensate in the x-z plane is an ellipse, the ratio between the two axis being equal to $\sqrt{\lambda}$. However the distribution corresponding to the excited particles will be spherical because of equipartition theorem. Therefore the anisotropy of the distribution is a strong evidence of BEC.

The above picture is modified by the two body interactions. Usually two extreme cases are taken into account that are distinguished by the ratio of the interaction and the kinetic energy which can be shown to be:

$$\frac{E_{\text{int}}}{E_{\text{kin}}} \propto \frac{N|a|}{d_0} \tag{5}$$

In the weakly interacting (near ideal) regime the above ratio is negligible and the wave function of the condensate is in good approximation the wave function of the non interacting gas 3.

In the strongly coupling limit (Thomas Fermi limit, TF) which is most relevant to the current experiments on BECs, $\frac{N|a|}{d_0} \gg 1$ and for a repulsive (attracive) interaction the resulting wave function turns out to difeer significantly from the gaussian and more specifically in is lowered (reaised) in the center and becomes wider (narrower). This can be justified by solving the Gross-Pitaevskii equation.

3 The Gross-Pitaevskii Equation

The Gross Pitaevskii equation is necessary for describing tha dynamics of a non uniform condensate and thus it is useful for describing both the case of trapped alkali gasses and also the occurence of vortices. The general idea behind that equation is that there is a macroscopic order parameter Ψ that describes the condensate which below the critical temperature and for a uniform condensate is simply $\Psi = \sqrt{N_0/V}$ which means that there is macrosopic occupation of the ground state with N_0 partiles and the rest $N' = N - N_0$ particles are distributed in the excited states with $\mathbf{k} \neq 0$. In the Bogoliubov approximation the ground state creation/annihilation operators are treated as numbers $a_0 \approx a_0^\dagger \approx \sqrt{N_0}$ because the ground state expectation value $\langle a_0^\dagger a_0\rangle = N_0$ is macroscopic and the occupation of the other states is less than 1. Non uniform states can be treated by using the hamiltonian

The existence of nonuniform states of a dilute Bose gas can be understood by considering a second-quantized Hamiltonian

$$\hat{H} = \int dV \left[\hat{\psi}^\dagger \left(T + V_{tr} \right) \hat{\psi} + g \hat{\psi}^\dagger \hat{\psi}^\dagger \hat{\psi} \hat{\psi} \right], \tag{6}$$

where $\hat{\psi}(\mathbf{r})$ and $\hat{\psi}^\dagger(\mathbf{r})$ are the usual field operators, $T = -\hbar^2 \nabla^2 / 2M$ is the kinetic energy operator for the particles , $V_{tr}(\mathbf{r})$ is an external (trap) potential, and the last term trepresents a short range interaction between the particles of the form $\approx g\,\delta(\mathbf{r}\text{-}\mathbf{r}')$. The coupling constant g for a dilute cold gas is related to the so called s-wave scattering length a by $g \approx 4\pi a \hbar^2 / M$[1]We can derive the Gross Pitaevskii equation by using the above Hamiltonian to generate the equation of motion of the Heisenberg operator $\hat{\psi}(\mathbf{r}, t)$

$$i\hbar \frac{\partial \hat{\psi}(\mathbf{r}, t)}{\partial t} = [\hat{\psi}(\mathbf{r}, t), \hat{H}] = (T + V_{tr})\, \hat{\psi}(\mathbf{r}, t) + g\, \hat{\psi}^\dagger(\mathbf{r}, t)\, \hat{\psi}(\mathbf{r}, t)\, \hat{\psi}(\mathbf{r}, t). \tag{7}$$

Then we take into account the macroscopic occupation of the ground state and substitute in the above $\hat{\psi}(\mathbf{r}, t) = \Psi(\mathbf{r}, t) + \hat{\phi}(\mathbf{r}, t)$ where $\Psi(\mathbf{r}, t)$ is the order parameter that characterizes the condensate and $\hat{\phi}(\mathbf{r}, t)$ is a a field operator referring to the noncondensed particles. Keeping only terms to zero order in $\hat{\phi}$ gives the so called time-dependent Gross Pitaevskii equation:

$$i\hbar \frac{\partial \Psi(\mathbf{r}, t)}{\partial t} = \left[T + V_{tr} + g\, |\Psi(\mathbf{r}, t)|^2 \right] \Psi(\mathbf{r}, t) \tag{8}$$

for the condensate wave function $\Psi(\mathbf{r}, t)$. The stationary solutions of this non linear "Schroediger-like" equation are obtained by substituting $\Psi(\mathbf{r}, t) = \Psi(\mathbf{r})\, e^{-i\mu t/\hbar}$, to get the stationary GP equation:

$$(T + V_{tr} + g|\Psi|^2)\Psi = \mu \Psi \tag{9}$$

Essentially all studies of trapped atomic gases involve the dilute limit ($\bar{n}|a|^3 \ll 1$, where $\bar{n}$ is the average density of the gas), so that depletion of the condensate is small with $N' = N - N_0 \propto \sqrt{\bar{n}|a|^3} N \ll N$. Typically $\bar{n}|a|^3$ is always less than 10^{-3}. Hence most of the particles remain in the condensate, and the difference between the condensate number N_0 and the total number N can usually be neglected. In this case, the stationary GP equation (9) for the condensate wave function follows by minimizing the Hamiltonian:

$$H = \int dV \left[\Psi^* \left(T + V_{tr} \right) \Psi + \frac{1}{2} g |\Psi|^4 \right] \tag{10}$$

subject to a constraint of fixed condensate number $N_0 = \int dV\, |\Psi|^2 \approx N$ (readily included with a Lagrange multiplier that is simply the chemical potential μ).

[1]Scattering lengths of atomic gasses frequently used in experiments are: $a = 2.75$ nm for ^{23}Na, $a = 5.77$ nm for ^{87}Rb, and $a = -1.45$ nm for ^{7}Li.

It is instructive to rewrite the GP using rescaled dimensionless variables. Let us consider a spherical trap with frequency ω_0 and use d_0, d_0^{-3} and $\hbar\omega_0$ as units of length, density and energy, respectively. By putting a tilde over the rescaled quantities, Eq. (9) becomes

$$\left[-\tilde{\nabla}^2 + \tilde{r}^2 + 8\pi(Na/d_0)\tilde{\phi}^2(\tilde{\mathbf{r}})\right]\tilde{\phi}(\tilde{\mathbf{r}}) = 2\tilde{\mu}\tilde{\phi}(\tilde{\mathbf{r}})$$

In these new units the order parameter satisfies the normalization condition $\int d\mathbf{r}|\tilde{\phi}|^2 = 1$. Obviously the only important parameter is Na/a_{ho}. It is worth noticing that the solution of the stationary GP equation (9) minimizes the energy functional (10) for a fixed number of particles and can be written as follows:

$$E[n] = \int d\mathbf{r}\left[\frac{\hbar^2}{2m}\left|\nabla\sqrt{n}\right|^2 + nV_{tr}(\mathbf{r}) + \frac{1}{2}gn^2\right] = E_{\mathrm{kin}} + E_{\mathrm{ho}} + E_{\mathrm{int}} \qquad (11)$$

The first term corresponds to the quantum kinetic energy coming from the uncertainty principle and is usually called "quantum pressure" and vanishes for uniform systems. The second term is the effect of the external potential and the third is a self consistent mean field potential coming from the distribution of particles.

The equilibrium of the quantum pressure and the mean potential gives rise to a length scale called "correlation" or "healing" length because it is a measure of how fast the order parameter heals back to its bulk value when perturbed localy (is in a vortex core):

$$\xi = \frac{1}{\sqrt{2Mng}} = \frac{1}{\sqrt{8\pi na}}$$

In case of trapped systems we can use the central density to get a magnitude for the healing lenght in which case: $\xi = [8\pi n(0)\,a]^{-1/2}$. In the TF limit, this choice implies that

$$\xi\, R_0 = d_0^2, \quad \text{or,equivalently,} \quad \frac{\xi}{d_0} = \frac{d_0}{R_0} \ll 1. \qquad (12)$$

Thus the TF limit provides a clear separation of length scales $\xi \ll d_0 \ll R_0$, and the (small) healing length ξ characterizes the small vortex core. In contrast, the healing length (and vortex-core radius) in the near-ideal limit are comparable with d_0 and hence with the size of the condensate.

We can use the Gross-Pitaevskii to investigate the profile of a single vortex. In order to simplify the analysis a little bit we only consider the two dimensional case of a uniform gas in which a vortex of strength 1 (the phase around it changes by 2π) is represented by a wave function of the form $\Psi(\mathbf{r}) = \sqrt{n}\,\chi(\mathbf{r})$, where n is the density of the condensate far from the origin and $\chi(\mathbf{r})$ is defined by:

$$\chi(\mathbf{r}) = e^{i\phi} f\left(\frac{r_\perp}{\xi}\right), \qquad (13)$$

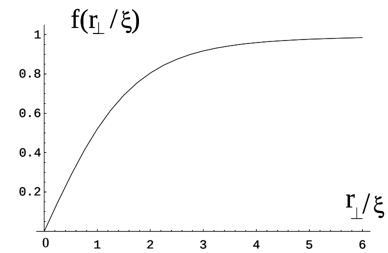

Figure 1: Radial wave function $f(r_\perp/\xi)$ obtained by numerical solution of the stationary GP equation for a straight vortex line.

The kinetic energy per unit length is given by

$$\int d^2r_\perp \Psi^* \left(-\frac{\hbar^2\nabla^2}{2M}\right)\Psi = \frac{\hbar^2}{2M}\int d^2r_\perp |\nabla\Psi|^2 = \frac{\hbar^2 n}{2M}\int d^2r_\perp \left[\left(\frac{df}{dr_\perp}\right)^2 + \frac{f^2}{r_\perp^2}\right] \tag{14}$$

From these equations we can see that the boundary conditions for f and more specifically $f \to 1$ for $r_\perp \gg \xi$ and the centrifugal barrier in the second term forces the amplitude to vanish linearly within a core of radius $\approx \xi$ (see Fig. 1). This core structure ensures that the particle current density $\mathbf{j} = n\mathbf{v}$ vanishes and the total kinetic-energy density remains finite as $r_\perp \to 0$. A numerical analysis of the GP equation can give us the energy of the vortex which is $E_v \approx (\pi\hbar^2 n/M)\ln(1.46R/\xi)$ where R is the size of the condensate. This comes from the kinetic energy of the flow circulating around the vortex and also the compression of the condensate close to the core. In the case of a trapped gas with a single vortex and axial symmetry the analysis is a bit more complicated. Rotational symmetry implies that the macroscopic wave function is of the form: If we consider an axisymmetric trap with oscillator frequencies ω_z and $\omega_\perp$ and axial asymmetry parameter $\lambda \equiv \omega_z/\omega_\perp$ the rotational symmetry suggests the following form of the wave function for a vortex of unit strength along the z axis:

$$\Psi(\mathbf{r}) = e^{i\phi}\,|\Psi(r_\perp, z)|. \tag{15}$$

The centrifugal energy [compare Eq. (14)] gives rise to an additional term $\frac{1}{2}Mv^2 = \hbar^2/2Mr_\perp^2$ in the GP equation (9).A vortex of strength q with $\Psi \propto e^{iq\phi}$ also satisfies the GP equation but its energy increases like q^2 which is larger than the energy of q vortices of unit strength. Therefore it will be unstable and collapse into unit vortices.

In general, the density for a central vortex vanishes along the symmetry axis, and the core radius increases away from the center of the trap, yielding a toroidal condensate density (see Fig. 2). This behavior is particularly evident for a vortex in the TF limit $Na/d_0 \gg 1$, when

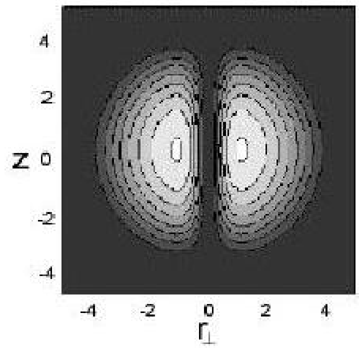

Figure 2: Contour plot in the xz plane for a condensate with 10^4 ^{87}Rb atoms containing a vortex along the z axis. The trap is spherical and distances are in units of the oscillator length $d = 0.791\mu$m. The interaction parameter is $Na/d = 72.3$. Luminosity is proportional to density, the white area being the most dense.

$$n(r_\perp, z) \approx n(0)\left(1 - \frac{\xi^2}{r_\perp^2} - \frac{r_\perp^2}{R_\perp^2} - \frac{z^2}{R_z^2}\right)\Theta\left(1 - \frac{\xi^2}{r_\perp^2} - \frac{r_\perp^2}{R_\perp^2} - \frac{z^2}{R_z^2}\right). \tag{16}$$

The density vanishes within a core whose characteristic radius is ξ in the equatorial region $|z| \ll R_z$ because of the term $\xi^2/r_\perp^2$. Then it flares out with increasing $|z|$. The TF separation of length scales ensures that the vortex affects the density only the immediate vicinity of the core; this behavior can usually be approximated with a short-distance cutoff. Now lets consider a condensate in equilibrium with a rotating trap at angular velocity Ω around the $\hat{z}$ axis. The hamiltonian density of Eq.(10) acquires an additional term $-\Psi^*\Omega L_z\Psi$ [?], where L_z is the usual z component of the angular-momentum operator. Thus the Hamiltonian H' in the rotating frame becomes

$$H' = H - \Omega L_z = \int dV \left[\Psi^*\left(T + V_{tr} - \Omega L_z\right)\Psi + \frac{1}{2}g|\Psi|^4\right] \tag{17}$$

where the variables in the integrand are now those in the rotating frame. Similarly, the GP equations (8) and (9) acquire an additional term $-\Omega L_z\Psi$.

In the case of an axissymmetric trap the states of the condensate can be labeled by L_z quantum number. For a vortex free condensate the ground state energy in the lab frame and in the rotated frame are equal because $(\Omega L_z)\,\Psi = 0$ and the expression of the energy is the same. For a vortex of unit strength $(\Omega L_z)\,\Psi = \hbar\Omega\Psi$ and the contribution of the Ω term is $N\hbar\Omega$, where $N\hbar$ is the total angular momentum of the condensate (N is the number of particles). Therefore $E_1'(\Omega) = E_1 - N\hbar\Omega$ and the difference between the two configurations in the rotated frame is:

$$\Delta E'(\Omega) = E_1'(\Omega) - E_0'(\Omega) = E_1 - E_0 - N\hbar\Omega \tag{18}$$

It is clear that $E_1 > E_0$ because of the added kinetic energy of the circulating flow. The existence of a vortex is not energetically preferable in the rotating frame up to acritical angular velocity where $\Delta E'(\Omega_c) = 0$:

$$\Omega_c = \frac{E_1 - E_0}{N\hbar}, \tag{19}$$

expressed solely in terms of energy of a condensate with and without the vortex evaluated in the laboratory frame.

For a noninteracting trapped gas, the difference is $E_1 - E_0 = N\hbar\omega_\perp$. This can be justfied by the fact that at $\Omega_c = \omega_\perp$ the centrifigural potential $-\frac{1}{2}M\Omega^2 r_\perp^2$ in the rotating frame is completely canceled by the radial trapping potential $\frac{1}{2}M\omega_\perp^2 r_\perp^2$. In a weakly interacting limit it can be shown that $\Omega_c/\omega_\perp$ decreases as the number of particle increases.

In the TF limit it can be shown that the critical velocity is given by:

$$\frac{\Omega_c}{\omega_\perp} \approx \frac{5}{2}\frac{d_\perp^2}{R_\perp^2}\ln\left(\frac{0.67R_\perp}{\xi}\right). \tag{20}$$

This ratio is small in the TF limit, because $d_\perp^2/R_\perp^2 \sim \xi/R_\perp \ll 1$. For an axisymmetric condensate with axial asymmetry $\lambda \equiv \omega_z/\omega_\perp$, the TF relation $d_\perp^2/R_\perp^2 = (d_\perp/15Na\lambda)^{2/5}$ shows how this ratio scales with N and λ.

4 Experimental observation of single vortex

The first experimental detection of a vortex involved a nearly spherical ^{87}Rb TF containing two different internal Rb spin states which were coupled with each other using external microwave radiation [4]. The topology of a two component system (the order parameter has two components) is rather different from this of a single component condensate. In the latter case it is a sphere and in the former a circle. This is because the apart from the magnitude $|\Psi|$ that is fixed by the temperature in a uniform system, a one-component order parameter has only the phase that varies between 0 and 2π whereas In contrast, a two-component system has two degrees of freedom in addition to the overall magnitude; one phase per component. The qualitative difference between the two cases can be understood as follows: the single degree of freedom of the one-component order parameter is like a rubber band wrapped around a cylinder, while the corresponding two degrees of freedom for the two-component order parameter is like a rubber band around the equator of a sphere. The former has a given winding number that can be removed only be cutting it (ensuring the quantization of circulation), whereas the latter can be removed simply by pulling it to one of the poles (so that there is no quantization).

The JILA group was able to spin up the condensate by coupling the two components. They then turned off the coupling, leaving the system with a

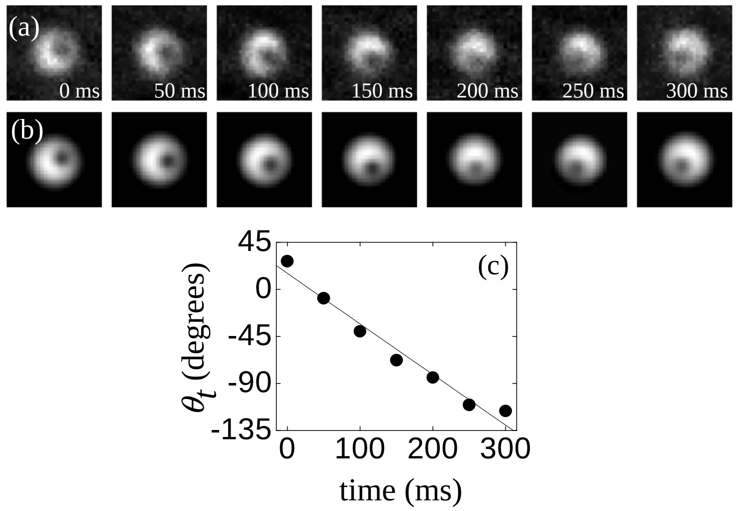

Figure 3: (a) Successive images of a condensate with a vortex. The recorded profile of each trapped condensate is fit with a smooth TF distribution (b). The vortex core is the dark region within the bright condensate image. (c) The azimuthal angle of the core is determined for each image, and plotted *vs.* time held in the trap. A linear fit to the data gives a precession frequency 1.3(1) Hz.

residual trapped quantized vortex consisting of one circulating component surrounding a nonrotating core of the other component, whose size is determined by the relative fraction of the two components. By selective tuning, they can image either component nondestructively; Fig. 3 shows the precession of the filled vortex core around the trap center. In addition, an interference procedure allowed them to map the variation of the cosine of the phase around the vortex, clearly showing the expected sinusoidal variation (Fig. 4).

Separately, the ENS group in Paris observed the formation of one and more vortices in a single-component ^{87}Rb elongated cigar-shape TF condensate [5]. The atomic condensate is stirred using an additional non axis-symmetric potential created by the dipole potential of a non resontan stirring laser beam. The combined potential produces a cigar-shape harmonic trap with a slightly anisotropic transverse profile. The transverse anisotropy rotates slowly at a rate $\Omega \approx 200$ Hz. The presence of the vortex is then revealed by a the density dip at the center of the spacial distribution of the condensate.

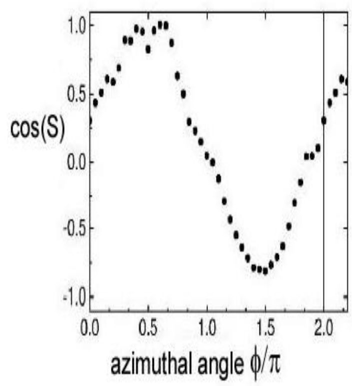

Figure 4: Cosine of the phase around the vortex, showing the sinusoidal variation expected for the azimuthal angle.

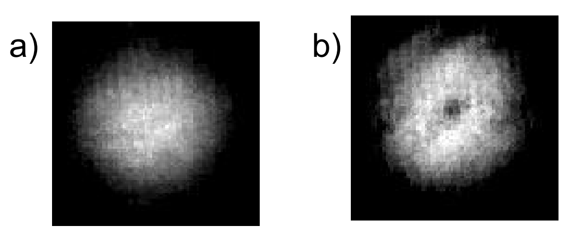

Figure 5: Optical thickness of the expanded clouds in the transverse direction showing the difference between the states (a) without and (b) with a vortex.

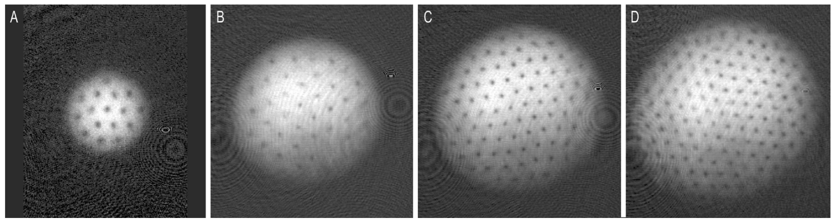

Figure 6: Observation of vortex lattices. The examples shown contain approximately (A) 16, (B) 32, (C) 80, and (D) 130 vortices. The vortices have "crystallized" in a triangular pattern. The diameter of the cloud in (D) was 1 mm after ballistic expansion, which represents a magnification of 20. Slight asymmetries in the density distribution were due to absorption of the optical pumping light.

5 Experimental observation of Vortex lattices

Vortex arrays have been observed in condensates that were subjected to steady rotation [6]. The vortex array that was created was rotating as a whole and simulates a rigid body rotation. In the following Figures the experimental results of Abo-Shaeers group are presented. They observed the formation of highly order triangular vortex lattices with remarkable stability. They contain over 100 vortices with lifetimes of about several seconds. The condensate was held in a magnetic trap and rotated under the influence of the dipole force from a laser beam. The vortex cores were probed using resonant absorption imaging after the confining potential was switched off. The observed "Abrikosov" lattices are characterized by the large number of vortices they can hold and also their extreme regularity even in the boundaries of the condensate.

6 Conclusions

Several aspects of the vorticity in alkali BECs can be studied using the GP equation. Open issues in the cotemporary theoretical and experimental work include the kinematics of vortex nucleation and decay, different methods for vortex creation and the study of vortices in BECs with attractive two body interactions. etc.

References

[1] A. L. Fetter A. A. Svidzinky, Vortices in trapped dilute Bose-Einstein Condensate, arxiv:cond-mat/0102003v1 1Feb2001.

[2] F. Dalfovo, S. Giorgini, Lev P. Pitaevskii, S. Stringari, Theory of Bose Einstein condensation in trapped gasses arxiv':cond-mat/9806038v2 12 Oct 1998.

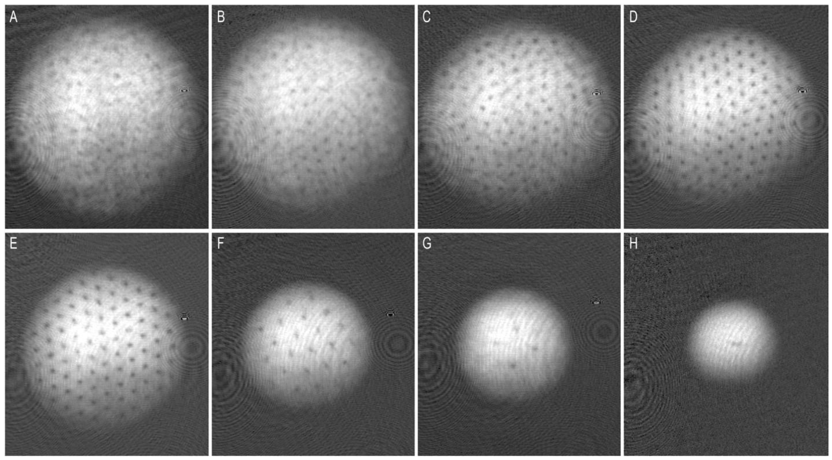

Figure 7: Formation and decay of a vortex lattice. The condensate was rotated for 400 ms and then equilibrated in the stationary magnetic trap for various hold times. (A) 25 ms, (B) 100 ms, (C) 200 ms, (D) 500 ms, (E) 1 s, (F) 5 s, (G) 10 s, and Image (H) 40 s. The decreasing size of the cloud in (E) to (H) reflects a decrease in atom number due to inelastic collisions. The field of view is ~1mm by 1.5mm.

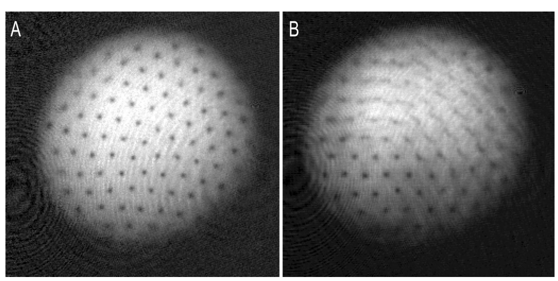

Figure 8: Vortex lattices with defects. In (A), the lattice has a dislocation near the center of the condensate. In (B), there is a defect reminiscent of a grain boundary.

[3] A. J. Legget, Bose-Einstein condensation in the alkali gasses: Some fundamental concepts, Review of Modern Physics, vol 73 No 2, p307.

[4] M. R. Matthews, B. P. Anderson, P. C. Haljan, D. S Hall, C. E. Wieman, and E. A. Cornell, Vortices in a Bose-Einstein condensate, Phys. Rev. Lett. 83, 2498 (1999)

[5] K. W. Madison, F. Chevy, W. Wohlleben, and J. Dalibard, Phys. Rev. Lett. 84 806 (2000)

[6] J. R. Abo-Shaeer, C. Raman, J. M. Vogels and W Ketterle, Observation of Vortex Lattices in Bose-Einstein condensates, Science 292: 476-479, March 22, 2001; 10.1126/scince. 1060182